Introduction: general setup and an example that forces chaos

Jan Bouwe van den Berg

November 22, 2015

Abstract

In this lecture the basic concepts of rigorous computing in a dynamical systems context will be outlined. We often simulate dynamics on a computer, or calculate a numerical solution to a partial differential equation. This gives very detailed, stimulating information. However, mathematical insight and impact would be much improved if we can be sure that what we see on the screen genuinely represents a solution of the problem. In particular, rigorous validation of the computations allows such objects to be used as ingredients of theorems.

The past few decades have seen enormous advances in the development of computer assisted proofs in dynamics. In this introductory talk we discuss the basic functional analytic setup underlying the rigorous computational method that is the central topic of this AMS short course. As the central example we will use the problem of finding a particular periodic orbit in a nonlinear ordinary differential equation that describes pattern formation in fluid dynamics. This simple setting keeps technicalities to a minimum. Nevertheless, the rigorous computation of this single periodic orbit implies chaotic behavior via topological arguments (in a sense very similar to "period 3 implies chaos" for interval maps [20]).

1 Introduction

These are concise lecture notes that accompany the introductory lecture of the AMS short course on Rigorous Numerics in Dynamics. This introduction starts with a few sections that are meant to provide motivation and general background information, and these are therefore of a rather global (and at times sketchy) nature. In §2 we turn to a precise mathematical formulation of the general analytic-computational approach. In §3 we introduce an example for which the approach is subsequently worked out in complete detail in §4. The main underlying references are [30] and [15].

1.1 Background: dynamical systems

Informally, a dynamical system is a system that evolves in time according to a deterministic law. The time variable $t \in \mathcal{T}$ may be either discrete or continuous. The time may flow forward ($\mathcal{T} = \mathbb{N}$ or $\mathcal{T} = \mathbb{R}^+ = [0, \infty)$) or forward-and-backward ($\mathcal{T} = \mathbb{Z}$ or $\mathcal{T} = \mathbb{R}$). It may happen that an evolution stops after some finite time (e.g. because it reaches infinity in finite time), but we will not be considering these (technical) details here. Mathematically, what we need are a topological space $\mathcal{X}$, the phase space, and a continuous function, the flow, $\varphi : \mathcal{X} \times \mathcal{T} \to \mathcal{X}$ with the properties

$$\varphi(x; 0) = x \qquad \text{for all } x \in \mathcal{X}, \tag{1a}$$

$$\varphi(x; t_1 + t_2) = \varphi(\varphi(x; t_1); t_2) \qquad \text{for all } x \in \mathcal{X} \text{ and } t_1, t_2 \in \mathcal{T}. \tag{1b}$$

The interpretation is that after a time t the state x has moved to $\varphi(x; t)$. The identity (1b) expresses that flowing for some time t_1 to a point $x_1 = \varphi(x; t_1)$ and then flowing another t_2 from x_1, gives the same result as flowing for a time $t_1 + t_2$ immediately.

One usually writes $x(t) = \varphi(x(0); t)$ if it is clear which flow is meant. The fundamental problem of dynamical systems is that in all but the simplest cases we do not know φ, i.e., we have no useful explicit description of the flow. However, there are many cases where a "law of motion" (for which we have an explicit description) together with initial data determine the entire future dynamics deterministically, hence we know there *is* a flow φ, i.e., it is a dynamical system.

Indeed, dynamical systems appear in all branches of sciences. To give a few examples:

- Physics: Newton's law of motion in classical mechanics
- Chemistry: the Schrödinger equation
- Fluid dynamics: the Navier-Stokes equations
- Economics: the Black-Scholes equation for option pricing
- Meteorology: coupled ocean-atmosphere models in weather forecasting
- Systems biology: reaction diffusion equations for reaction networks
- Astronomy: star-, planet-, and galaxy-, cluster-formation and their evolution
- Neuroscience: dynamic models for bursting neurons

Dynamical systems do not just occur in applications. Indeed, they are interesting from a mathematical perspective in their own right. Moreover, they appear in many branches of mathematics, such as in the Calculus of Variations (gradient flows), in differential geometry (e.g. the Ricci flow, leading, eventually, to the resolution of the Poincaré conjecture), in evolutionary and stochastics partial differential equations, and in symplectic geometry (pseudoholomorphic curves).

The modern theory of dynamical systems dates back to Poincaré and his study of the (in)stability of the solar system and its ultimate fate. More generally, the central question in dynamical systems is the following: start at some point $x(0)$ and let it evolve under the flow φ; *now what happens?* And how do the individual orbits fit together to give a global description of the behavior of the system as a whole? Additionally, one would like to know not just how the ultimate fate depends on the initial position, but also on parameters in the system, and on the "type" of system (e.g. Hamiltonian, gradient, symmetric, network structure).

Clearly, no single method can answer all these questions, especially since there are so many types of dynamical systems (linear, nonlinear, ordinary differential equations (ODEs), partial differential equations (PDEs), delay equations, finite and infinite dimensional maps).

Linear dynamical systems can often be analyzed by hand using linear algebra, functional analysis and special functions. In this short course we are interested in *nonlinear* dynamics, for which the analytic tools are much coarser: topological approaches (e.g. fixed point theorems, Conley index) and variational methods (e.g. Morse theory) give some information about existence of solutions for large classes of systems, but for specific nonlinear dynamical systems such robust but coarse results lack information about multiplicity of solutions and there is usually very little qualitative (let alone quantitative) information about the shape of the solutions.

In practice, this is complemented by computer simulations, which give insight in the behavior of solutions, but there is unquantified uncertainty in this information due to the absence of explicit error bounds on the outcome of numerics. These errors originate from rounding errors and, more importantly, truncation and discretization errors.

The goal of the short course is to introduce a framework in which the quantitative but tentative information from computer simulations can be turned into mathematically rigorous statements (theorems). Numerical (computer) computations are naturally limited to a relatively small range of parameter values and a restricted part of phase space. In particular, our methods focus on rigorously (in the mathematical sense) finding solutions in nonlinear dynamical systems that represent *special features*. One may think of equilibria, cycles, connection orbits (homoclinic or heteroclinic), horseshoes ("chaos"), invariant tori, etc.

What the special solutions of most interest are will depend on the dynamical system, and in general one can only be vague about it. Nevertheless, some useful global statements can be made. In particular, in dissipative systems all dynamics will evolve towards an *attractor*, and hence studying this attractor is of most interest. More generally, the fundamental theorem of dynamical systems, due to Conley [7], states that any flow (on a compact metric space) decomposes into a *chain recurrent* part and a *gradient-like* part. The recurrent components consist, roughly speaking, of points that come back arbitrarily close to themselves under the evolution of the flow, whereas

points in the gradient part do not. The dichotomy is thus that points are either recurrent, or they run "downhill" towards a recurrent component (and if we can go back in time: they come from *another* recurrent component). It is thus interesting to study recurrent components as well as the connecting (heteroclinic) orbits between them. As an example, in a gradient flow the principle interest is in the (hyperbolic) equilibria and the heteroclinic orbits that connect equilibria with Morse index difference one.

1.2 Rigorous numerics

Computer assisted proofs have a relatively short history in mathematics. Nevertheless, the proof of the four color theorem [22] and of the densest sphere packing (Kepler problem) [14] belong to the classics in the field. Regarding the role of computers in dynamical systems, the start of the systematic study of nonlinear dynamical systems coincided with the advent of the computer (Feigenbaum diagram, Mandelbrot set). Although some qualitative properties were already sketched by Poincaré and contemporaries, only with the help of numerical simulations people were able to imagine and map the variety of dynamics exhibited by nonlinear systems. Ever since, computers have been a crucial instrument in the mathematical analysis of dynamical systems, providing both inspiration and a way to test (and reject) conjectures. Moreover, due to the very limited availability of tools for doing quantitative nonlinear analysis by hand, computers have been used as proof-assistents very early on. Prime examples are the proof of the universality of the Feigenbaum constant [18] and the existence of the (numerically "obvious") chaotic attractor in the Lorenz system [29].

By now there is a variety of computational frameworks that aid in the study of nonlinear dynamics. Each of these involves a combination of topological (or analytic-topological) arguments with (interval arithmetic) computations. In this short course we delve into the wealth of possibilities of one approach. Nevertheless, it is important to stress that there is a range of partly overlapping methodologies, each with their own strengths and relative weaknesses. To name a few (very briefly; we refer the reader to the references for examples and more details):

- Piotr Zgliczynski and collaborators have developed a method based on integrating the flow using rigorous enclosures and Taylor methods, combined with topological arguments (Conley index, covering relations) and derivative information (through so-called cone conditions) [34, 35]. An extensive C++ package CAPD (Computer Assisted Proofs in Dynamics) is available for supporting these proofs [5].

- Hans Koch, in collaboration with Gianni Arioli, has developed a general functional analytic approach to computer-assisted proofs in nonlinear analysis (e.g. [2, 3]). That work has provided the crucial underlying ideas for the techniques discussed in this short course.

- In a spirit similar to the above method, techniques have been developed for studying elliptic problems by combining a Newton-like fixed point map with computer-assisted computations with a variable mix of functional analytic and computational effort (e.g. [4, 21]). This forms another stepping stone for the techniques discussed in this short course.

- Konstantin Mischaikow and collaborators have developed a "database" approach to representing the global behavior of parameterised families of nonlinear dynamical systems [1, 17]. The database encodes the minimal Morse-Conley graphs and their dependence on parameters. This framework focusses on global dynamics while working up to a finite resolution. It hence complements the local but "infinitesimal" results that form the core of this short course.

The method described in these notes has been developed in the past decade by a number of people, and we refer to [6, 9, 10, 12, 19, 32, 33] and the references therein for a limited sample of the contributions.

1.3 Forcing theorems

Forcing theorems in dynamical systems are statements of the form: if there exists a solution (orbit) of type A, then there must be orbits of types B, C and D. In the most interesting cases, the list of implied orbits is infinitely long. These forcing theorems are strong tools in the study of nonlinear dynamics. The main obstacle to applying them in concrete situations is that it is usually very difficult to show that an orbit of type A exists, even if numerical simulations may be tentatively convincing. This is the perfect setting for showcasing the power of rigorous computations.

Examples of forcing theorems are (roughly in increasing order of sophistication)

- In scalar autonomous ordinary differential equations: if there are two equilibria then there exists a heteroclinic orbit (non necessarily between these equilibria), or (in very degenerate situations) a continuum of equilibria.
- In a planar system of ODEs: a periodic orbit implies the existence of an equilibrium (located inside the orbit). This is a classical result, where the forcing is via index theory.
- Interval maps: "period 3 implies chaos" [20]. If there exists a periodic orbit of (minimal) period 3, then there are periodic orbits of arbitrary period (this generalizes to the Sharkovsky ordering [25]) and there is an invariant set on which the dynamics is chaotic (has positive entropy with respect to a suitably defined distance).
- Three dimensional systems of ODEs: a Shilnikov homoclinic orbit (to an equilibrium with a one-dimensional unstable manifold and a two-dimensional 'spiral' stable manifold) implies chaos if the expansion rate of the unstable manifold is larger than the contraction rate in the stable manifold [26].
- Maps on two-dimensional manifolds: a periodic orbit whose associated braid (after suspension) is of pseudo-Anosov type implies chaotic dynamics for the map [28].
- Second order Lagrangian system: certain periodic orbits (to be made explicit in Section 3) imply chaos [13].
- In variational problems: the Morse-Floer homology encodes forcing relations between equilibria with certain (Morse-Floer) indices and connecting (heteroclinic) orbits between such equilibria [24].

2 The general setup

2.1 Motivation: Newton's method

If we numerically try to find a solution of $f(x) = 0$, where $f : \mathbb{R}^n \to \mathbb{R}^n$ is some nonlinear problem, then, starting from with some initial guess x_0, we may iterate the Newton scheme

$$x_{n+1} = \widetilde{T}(x_n) \stackrel{\text{def}}{=} x_n - Df(x_n)^{-1} \cdot f(x_n)$$

to obtain a sequence that hopefully approaches a zero of f quickly. Since

$$D\widetilde{T}(x)y = y - (D[Df(x)^{-1}]y) \cdot f(x) - Df(x)^{-1} \cdot Df(x) \cdot y$$

we find that $D\widetilde{T}(\hat{x})y = 0$ for any $\hat{x}$ such that $f(\hat{x}) = 0$, provided $Df(\hat{x})$ is invertible. This implies that if $Df(\hat{x})$ is invertible, then $\|D\widetilde{T}(x)\|$ is small near the fixed point $\hat{x}$, hence $\widetilde{T}$ is a contraction mapping with very strong contraction rate. If we merely want a (moderately strong) contraction mapping (e.g. because we rely on analytic arguments in addition to computer calculations), then there is thus quite a lot of room to alter the definition of the map $\widetilde{T}$ and still be successful. For example, one may try replacing $Df(x)^{-1}$ by $Df(x_0)^{-1}$ so that there is no need to recompute the inverse after every iteration.

2.2 Setup

Our approach starts by recasting the dynamic problem of interest as a zero finding problem $F(x) = 0$ in some *infinite* dimensional space. To fix ideas, let X and X' be Banach spaces, and $F : X \to X'$ is a (Fréchet) differentiable map (in practice: $F \in C^1(X, X')$ or $C^2(X, X')$). Assume that $\overline{x} \in X$ is an approximate zero of F, i.e. $\|F(\overline{x})\|_{X'} \approx 0$, and that we have a left inverse $DF(\overline{x})^{-1}$ of $DF(\overline{x})$. Then we can define the Newton-like map

$$\widehat{T}(x) = x - DF(\overline{x})^{-1}F(x).$$

If, as is explicitly assumed, $DF(\overline{x})$ is invertible, then fixed points of $\widehat{T}$ are in one-to-one correspondence with zeros of F. In this case we can attempt to show that $\widehat{T}$ is a contraction mapping in a neighborhood of $\overline{x}$. However, in practice inverting $DF(\overline{x})$ is "too difficult".

Thus we make use of an approximate inverse, typically obtained in part by computing a numerical inverse. We approximate $DF(\overline{x})$ by a (simpler) linear operator $A^\dagger : X \to X'$ and choose $A \in L(X', X)$ to be an approximate left inverse of $A^\dagger$.

In this computational framework the choice of the linear operator A is based on a computer calculation (a non-rigorous one). Namely, we choose (Galerkin) projections π and π' of X and X' onto N-dimensional subspaces X_N and X'_N, respectively, for some $N \in \mathbb{N}$. The natural embedding of X_N into X is denoted by ι. The finite dimensional truncated problem is then given by

$$0 = F_N(x_N) \stackrel{\text{def}}{=} \pi'_N F(\iota x_N),$$

where $F_N : X_N \to X'_N$ and $x_N \in X_N$. We then seek a numerical approximation $\overline{x}_N$ of a solution to $F_N(x_N) = 0$, for example using a (finite dimensional) Newton iteration scheme. The idea is that $\overline{x} \stackrel{\text{def}}{=} \iota\overline{x}_N$ is an approximate solution of $F(x) = 0$.

Next we compute the Jacobian $DF_N(\overline{x}_N)$ and determine a numerical inverse $A_N \approx DF_N(\overline{x}_N)^{-1}$. We now need to "extend" the operator $A_N : X'_N \to X_N$ (or $\iota A_N : X'_N \to X$) to an *injective* operator $A : X' \to X$. How one goes about making this extension depends on the problem. It should be simple enough to allow for explicit analysis, while accurate enough to be an "approximate" left inverse of $DF(\iota\overline{x}_N)$ in a sense that will be made precise in §2.3.

We then define the Newton-like operator

$$T(x) \stackrel{\text{def}}{=} x - AF(x). \tag{2}$$

Observe that if A is injective, then fixed points of T correspond to zeros of F. Our goal is to show that T is a contraction map on a ball around $\overline{x}$. This ball should not be chosen too small (since then it won't contain a zero of F), but neither should it be chosen too large (since one cannot prove that T is a contraction on such larger balls (in fact it might not *be* a contraction there)).

Remark 1. *The space X' has no significance. The only important requirement is that we choose a linear operator A such that $AF(x) \in X$ for all $x \in X$.*

Remark 2. *To have correspondence between fixed points of T and zeros of F, we need that $AF(x) = 0$ implies $F(x) = 0$, i.e., A is injective on the range of F. In fact, one only needs that A is injective on the range of F when the domain of F is restricted to the fixed point space of T (e.g., one may have a priori knowledge about this due to symmetries).*

2.3 The theorem

The following theorem provides conditions under which we can guarantee the existence of a fixed point of T (and hence a zero of F provided A is injective).

Let X be a Banach space. Let $B_r(\overline{x})$ denote the *closed* ball of radius r around $\overline{x} \in X$.

Theorem 3. *Let T be a Fréchet differentiable map from a Banach space X to itself, such that for all $r \geq 0$*

$$\|T(\overline{x}) - \overline{x}\|_X \leq Y \tag{3a}$$

$$\|DT(x)\|_{B(X)} \leq Z(r) \qquad \text{for all } x \in B_r(\overline{x}), \tag{3b}$$

for some $Y \in \mathbb{R}^+$ and some function $Z : \mathbb{R}^+ \to \mathbb{R}^+$. If there exists an $\hat{r} > 0$ such that

$$Y + \hat{r}Z(\hat{r}) < \hat{r}, \tag{4}$$

then T has a unique fixed point in $B_{\hat{r}}(\overline{x})$.

The proof of the theorem is given in §2.5. We note that this is an abstract theorem in the sense that does not immediately reveal the context of §2.2. However, one should keep in mind that the bounds Y and $Z(r)$ will be given by complicated but explicit formulas that depend on numerically obtained values, see §4 for a detailed example. Indeed, both A (which appears in the definition (2) of T) and $\overline{x}$ are determined (largely) numerically. The inequality (4) is then checked with the help of a computer by using interval arithmetic. In practice Z usually depends polynomially on r. We then denote the so-called *radii polynomial* by

$$p(r) \stackrel{\text{def}}{=} Y + r[Z(r) - 1],$$

and we look for an $\hat{r} > 0$ such that $p(\hat{r}) < 0$. We note that we keep r as a variable parameter at the cost of having to work with a functional form for $Z = Z(r)$, which requires careful bookkeeping. The advantage is that we have more flexibility, not just enhancing the chance of proving that a fixed point of T exists, but also allowing better bounds both on the location of the fixed point (by determining the smallest $\hat{r}$ for which $p(\hat{r})$ is negative) and on the uniqueness range (by determining the largest $\hat{r}$ for which $p(\hat{r})$ is negative).

One may interpret (3a) as an estimate of the residue (but observe that the residue is "pre-conditioned" with the linear operator A), while (3b) represents both a bound on how well A approximates $DF(\overline{x})^{-1}$ and an estimate of how nonlinear the problem is.

On the one hand, one may view Theorem 3 as a mathematically rigorous form of an explicit a-posteriori error analysis. On the other hand, it represent the widely used approach in analysis of setting up a fixed point problem on some ball around a guess for the solution, using a "suitable choice" of a linear operator (denoted by A in our case). In our context, the formulation is adjusted to a situation where both the (center of the) ball and the linear operator depend heavily on numerically obtained values.

Since the theorem gives uniqueness, it is clear that one can only attack problems that are formulated in such a way that they have isolated solutions. Moverover, since the solution is obtained from a contraction argument (see §2.5), the solution is stable under small perturbations of the problem, hence only robust solutions can be found, and only problems with robust solutions can be analyzed. Often this requirement can be achieved by carefully reformulating the problem, after understanding the sources of non-uniqueness and/or non-robustness. This robustness feature should also be viewed as an advantage, since if one finds a solution then it is automatically "in general position" (e.g. hyperbolic or transversal), a property that is often required when using it as an ingredient in a larger mathematical context, such as in forcing theorems. Moreover, the setup is perfect for performing continuation in parameters, which is of crucial importance in most applications of nonlinear dynamical systems.

2.4 Alternative formulations

Since $T(x) = x - AF(x)$, the conditions (3a) and (3b) may be reformulated in terms of F. Furthermore, in practice the estimate on DF is split into three components with the help of an operator $A^\dagger$ that approximates $DF(\overline{x})$. The conditions (3) are then replaced by

$$\|AF(\overline{x})\|_X \leq Y \tag{5a}$$

$$\|I - AA^\dagger\|_{B(X)} \leq Z^0 \tag{5b}$$

$$\|A[A^\dagger - DF(\overline{x})]\|_{B(X)} \leq Z^1 \tag{5c}$$

$$\|A[DF(x) - DF(\overline{x})]\|_{B(X)} \leq Z^2(r) \qquad \text{for all } x \in B_r(\overline{x}), \tag{5d}$$

for some Y, Z^0, $Z^1 \in \mathbb{R}^+$ and $Z^2 : \mathbb{R}^+ \to \mathbb{R}^+$, and one sets $Z(r) = Z^0 + Z^1 + Z^2(r)$. The final estimate (5d) is often replaced by a Lipschitz bound

$$\|A[DF(x) - DF(x')]\|_{B(X)} \leq \widehat{Z}^2 \|x - x'\| \qquad \text{for all } x, x' \in B_{r^*}(\overline{x}),$$

where $r^* > 0$ is some a priori bound on the radius, and $Z^2(r) = \widehat{Z}^2 r$. The Lipschitz bound may, in turn, be supplanted by a bound on the second derivative:

$$\|AD^2F(x)[v, w]\|_X \leq \widehat{Z}^2 \qquad \text{for all } v, w \in B_1(\overline{x}) \text{ and all } x \in B_{r^*}(\overline{x}).$$

In both cases one needs an a posteriori check that the radius $\hat{r}$ for which $p(\hat{r}) < 0$ also satisfies $\hat{r} \leq r^*$. In this notation the radii polynomial is written as

$$p(r) = Y + r[Z^0 + Z^1 - 1] + r^2 \widehat{Z}^2 \qquad \text{for } r \in [0, r^*].$$

When we find a radius $\hat{r} \leq r^*$ such that $p(\hat{r}) < 0$, and if we know that A is injective, then we conclude that F has a unique zero in $B_{\hat{r}}(\overline{x})$. As mentioned before, the smallest such $\hat{r}$ gives the best bound on where the solution is, whereas the biggest such $\hat{r}$ gives the strongest uniqueness result.

2.5 The proof of Theorem 3

The goal is to show that T is a uniform contraction on $B_{\hat{r}}(\overline{x})$. First, we check that $B_{\hat{r}}(\overline{x})$ gets mapped into itself. Let $x \in B_{\hat{r}}(\overline{x})$ and apply the Mean Value Theorem for Banach spaces to obtain

$$\begin{aligned} \|T(x) - \overline{x}\|_X &\leq \|T(x) - T(\overline{x})\|_X + \|T(\overline{x}) - \overline{x}\|_X \\ &\leq \sup_{x' \in B_{\hat{r}}(\overline{x})} \|DT(x')\|_{B(X)} \|x - \overline{x}\|_X + Y \\ &\leq Z(\hat{r})\hat{r} + Y. \end{aligned}$$

Since $Z(\hat{r})\hat{r} + Y < \hat{r}$ by assumption, it follows that that T maps $B_{\hat{r}}(\overline{x})$ into itself. Second, to see that T is a contraction on $B_{\hat{r}}(\overline{x})$, let $x_1, x_2 \in B_{\hat{r}}(\overline{x})$ be arbitrary, and use the estimate (again applying the Mean Value Theorem)

$$\|T(x_1) - T(x_2)\|_X \leq \sup_{x' \in B_{\hat{r}}(\overline{x})} \|DT(x')\|_{B(X)} \|x_1 - x_2\|_X \leq Z(\hat{r}) \|x_1 - x_2\|_X. \tag{6}$$

It follows readily from $Y + Z(\hat{r})\hat{r} < \hat{r}$ with $Y \geq 0$ that the contraction rate $Z(\hat{r})$ in (6) is less than unity. Applying the Banach contraction mapping theorem finishes the proof.

3 Example of a rigorous computation that forces chaos

The following description in §3 is largely taken verbatim from the paper "Chaotic braided solutions via rigorous numerics: chaos in the Swift-Hohenberg equation" by Jan Bouwe van den Berg and Jean-Philippe Lessard [30].

We focus our attention on the Swift-Hohenberg equation, a fourth order parabolic partial differential equation (PDE), traditionally written as

$$\frac{\partial U}{\partial T} = -\left(\frac{\partial^2}{\partial X^2} + 1\right)^2 U + \alpha U - U^3, \tag{7}$$

which is widely used as a model for pattern formation due to a finite wavelength instability, such as in Rayleigh-Bénard convection (e.g., see [8, 27]). The onset of instability is at $\alpha = 0$. Stationary profiles satisfy the ODE

$$-U'''' - 2U'' + (\alpha - 1)U - U^3 = 0, \tag{8}$$

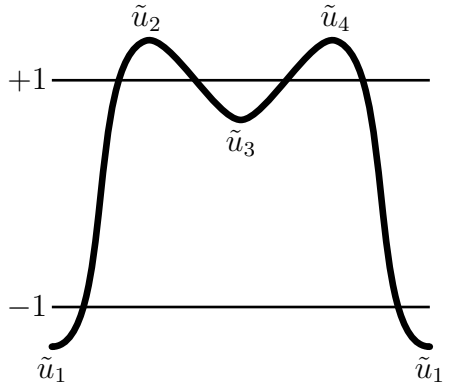

Figure 1: Sketch of a periodic solution $\tilde{u}$ satisfying the geometric properties $\mathcal{H}$.

which has a constant of integration, called the *energy*

$$E = U'''U' - \frac{1}{2}U''^2 + U'^2 - \frac{\alpha-1}{2}U^2 + \frac{1}{4}U^4 + \frac{(\alpha-1)^2}{4},$$

which has been normalized so that, for $\alpha > 1$, the nontrivial homogeneous states $U = \pm\sqrt{\alpha-1}$ have energy $E = 0$. The dynamics of (8) have been studied extensively, especially for small $\alpha > 0$, but many questions remain open for larger values of the parameter. Numerical simulations suggest chaotic behavior of (8) for most (or all) $\alpha > 0$.

The energy level $E = 0$ is special in the sense that it is a singular energy level, and it contains the nontrivial homogeneous states $U = \pm\sqrt{\alpha-1}$. Those equilibria are stable solutions of the PDE (7) for $\alpha > \frac{3}{2}$, and saddle-foci for the ODE (8) in the same parameter range. It is well known that saddle-foci may act as organizing centers for complicated dynamics [11, 16], and this inspires us to focus our attention on the dynamics in the energy level $E = 0$. The main result is that the Swift-Hohenberg ODE has chaotic dynamics in the energy level $E = 0$ for a large (continuous) range of parameter values.

Proposition 4. *The dynamics of the Swift-Hohenberg ODE* (8) *on the energy level* $E = 0$ *is chaotic for all* $\alpha \geq 2$.

Before we discuss the method of proof, let us comment that the parameter range $\alpha \geq 2$ can be extended somewhat using our method, but certainly not to cover the entire range $\alpha > 0$, as will be explained below.

Rather than working directly with (8) we first perform a change of coordinates that compactifies the parameter range, as well as making the notation more convenient. The new variables are

$$y = \frac{X}{\sqrt[4]{\alpha-1}}, \qquad u(y) = \frac{U(X)}{\sqrt{\alpha-1}}, \qquad \xi = \frac{2}{\sqrt{\alpha-1}}. \tag{9}$$

The parameter range $\alpha \geq 2$ corresponds to $\xi \in (0, 2]$, and the differential equation becomes

$$-u'''' - \xi u'' + u - u^3 = 0, \tag{10}$$

while the expression for the energy is now

$$E = u'''u' - \frac{1}{2}u''^2 + \frac{\xi}{2}u'^2 + \frac{1}{4}(u^2-1)^2. \tag{11}$$

In the method presented here, chaos is forced by the existence of a *single* periodic solution $\tilde{u}$ with specific geometric properties, much like a period-3 solution of an interval map implies chaos [20]

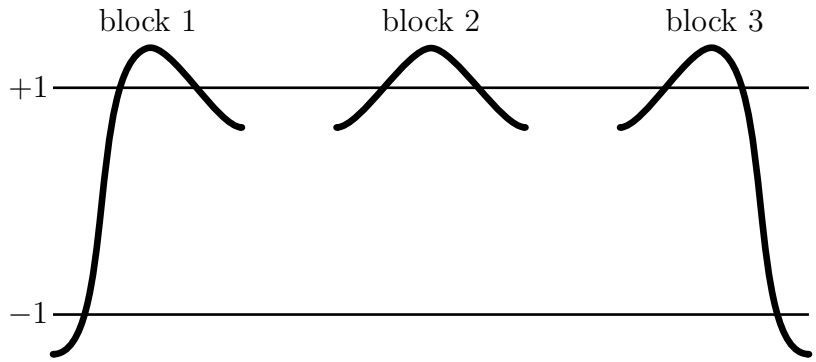

Figure 2: Building blocks for the solutions that lead to the chaos of Theorem 5.

(or a pseudo-Anosov braid in the context of surface homeomorphisms [28]). The periodic solution we are looking for needs to satisfy the following geometric properties, see also Figure 1:

$$\mathcal{H}\ \begin{cases} (H_1)\ \ \tilde{u} \text{ has exactly four monotone laps and extrema } \{\tilde{u}_i\}_{i=1}^4; \\ (H_2)\ \ \tilde{u}_1 \text{ and } \tilde{u}_3 \text{ are minima, and } \tilde{u}_2 \text{ and } \tilde{u}_4 \text{ are maxima;} \\ (H_3)\ \ \tilde{u}_1 < -1 < \tilde{u}_3 < 1 < \tilde{u}_2, \tilde{u}_4; \\ (H_4)\ \ \tilde{u} \text{ is symmetric in its minima } \tilde{u}_1 \text{ and } \tilde{u}_3. \end{cases}$$

Let the extrema $\tilde{u}_i$ be attained in $\tilde{y}_i$, then the last condition can be reformulated as

$$\tilde{u}(\tilde{y}_1 + y) = \tilde{u}(\tilde{y}_1 - y) \qquad \text{and} \qquad \tilde{u}(\tilde{y}_3 + y) = \tilde{u}(\tilde{y}_3 - y).$$

In particular, it implies that $\tilde{u}_2 = \tilde{u}_4$. We should note that condition H_4 is in fact not necessary for the results below to hold, but it simplifies the exposition.

As said before, such periodic solutions can be used to prove chaos when the equilibria $u = \pm 1$ are saddle-foci, i.e., when $\xi < \sqrt{8}$.

Theorem 5 (forcing)**.** *Let $\xi \in [0, \sqrt{8})$, and suppose there exists a periodic solution $\tilde{u}$ of* (10) *at the energy level $E = 0$, satisfying the geometric conditions $\mathcal{H}$. Then* (10) *is chaotic on the energy level $E = 0$ in the sense that there exists a two-dimensional Poincaré return map which has a compact invariant set on which the topological entropy is positive.*

The construction of the chaotic invariant set hinges on an application of Conley index theory for discretized braids [13, 30]. Let us briefly discuss some intuition behind the result. The set of solutions of (10) that leads us to chaotic dynamics is obtained by putting the three building blocks in Figure 2 together. The order of the blocks should follow the intuition coming from Figure 2, i.e., blocks 1 and 2 may be followed by block 2 or 3, while block 3 can only be followed by block 1. The sequence of building blocks may be chosen arbitrarily as long as these rules are obeyed, and the different possibilities are sufficiently complicated to lead to chaos. The final technical step in proving chaos is then to find a semi-conjugacy to a subshift of finite type, see [30, §2]. Furthermore, we note that all the solutions to the ODE (10) built from these building blocks correspond to equilibria of the PDE (7) that are *stable* under the evolution of the PDE. Hence, this result has significant implications for the pattern forming properties of the Swift-Hohenberg PDE.

It is important to note that the only hypothesis that needs to be verified in order to prove the existence of chaos in (10) at $E = 0$ is the existence of a *single* periodic solution $\tilde{u}$ satisfying $\mathcal{H}$. This will be done via rigorous numerics, i.e. computer assisted (interval arithmetic) calculations, together with a set of analytic estimates of the "tail" terms, i.e., the remainder terms not covered by the finite dimensional reduction. The construction leads to the existence of the periodic solution with the required geometric properties for a large range of parameter values.

Theorem 6 (rigorous computation)**.** *For every $\xi \in [0,2]$ equation* (10) *has a periodic solution at energy level $E = 0$ satisfying the geometric properties $\mathcal{H}$.*

The change of variables (9) directly converts Theorems 5 and 6 into Proposition 4.

Numerical simulations suggest that although the parameter range in Theorem 6 (and hence Proposition 4) can be increased somewhat, the solution $\tilde{u}$ with the described geometric behavior in fact disappears in a saddle node bifurcation at some critical value $\xi_* > 2$ ($\xi_* \approx 2.03$, see also [31]). Hence, one has to find a different mechanism to force chaos if one wants to prove a similar result for the parameter range $\xi > \xi_*$.

In this introductory lecture we will give part of the proof of Theorem 6. In particular we will discuss all details of how to prove that for *fixed* parameter value ξ equation (10) has a periodic solution at energy level $E = 0$ satisfying, see §4. These solutions will satisfy the geometric properties $\mathcal{H}$, but we will not discuss how to check that rigorously. Since the method provides a *quantitative* description of the solution with a small *explicit* error bound, it is relatively easy to check the geometric properties $\mathcal{H}$. We refer to [30, §4] for the details.

One can also prove the result for a *continuous* range of ξ-values, see [30] for the details, but we have chosen not to burden the exposition with this. Instead, we postpone discussion of continuation techniques to one of the later lectures in this short course. Additionally, we will not discuss the proof of the forcing Theorem 5 as it requires methods that are disjoint from the aims of the short course; we refer the interested reader to [30, §2].

4 The computational proof

We will first convert the problem of finding a periodic solution to Fourier space (§4.1). Then we introduce a convenient norm on the space Fourier coefficients (§4.2). The full problem consists of the ODE (10) and the energy constraint $E = 0$, with the Fourier coefficients and the frequency as variables. In §4.3 we reformulate this as a fixed point problem of the type (2). In particular, we define finite dimensional projections and the linear operator A. The radii polynomials for the problem are defined in §4.4, and we formulate the existence theorem. Explicit expressions for the necessary bounds Y and Z are derived in §4.5 and §4.6, respectively. Finally, the matlab code that clinches the proof is discussed briefly in §4.7.

4.1 Fourier transform

We are going to restrict our attention to symmetric periodic solutions u satisfying $\mathcal{H}$, hence we expand u as a cosine series:

$$u(y) = a_0 + 2\sum_{m=1}^{\infty} a_m \cos(mqy), \tag{12}$$

with $q > 0$ an *a priori unknown* variable ($\frac{2\pi}{q}$ is the period) and $a_m \in \mathbb{R}$ for $m \geq 0$. One may also think of this as

$$u(y) = \sum_{m\in\mathbb{Z}} a_{|m|} e^{imqy}, \tag{13}$$

i.e., the Fourier transform with symmetry constraint $a_{-m} = a_m$.

Since $u'(0) = 0$, and since the energy (11) is a conserved quantity along the orbits of (10), we get that

$$\begin{aligned} E &= u'''(0)u'(0) - \frac{1}{2}u''(0)^2 + \frac{\xi}{2}u'(0)^2 + \frac{1}{4}(u^2-1)^2 \\ &= -\frac{1}{2}\left[u''(0) - \frac{1}{\sqrt{2}}\big(u(0)^2-1\big)\right]\left[u''(0) + \frac{1}{\sqrt{2}}\big(u(0)^2-1\big)\right]. \end{aligned}$$

We look for u such that $E = 0$, $u(0) < -1$ and $u''(0) > 0$, hence the energy condition boils down to

$$u''(0) - \frac{1}{\sqrt{2}}[u(0)^2 - 1] = 0. \tag{14}$$

Substituting the expansion (12) for $u(y)$ in (14), we obtain

$$f_q(q,a) \stackrel{\text{def}}{=} -2q^2 \sum_{m=1}^{\infty} m^2 a_m - \frac{1}{\sqrt{2}} \left[a_0 + 2 \sum_{m=1}^{\infty} a_m \right]^2 + \frac{1}{\sqrt{2}} = 0. \tag{15}$$

In Fourier space the ODE (10) converts into an infinite sequence of algebraic equations:

$$(f_a)_k(q,a) \stackrel{\text{def}}{=} -\lambda_k(q) a_k - \sum_{\substack{k_1+k_2+k_3=k \\ k_i \in \mathbb{Z}}} a_{|k_1|} a_{|k_2|} a_{|k_3|} = 0 \qquad \text{for all } k \geq 0, \tag{16}$$

where

$$\lambda_k(q) \stackrel{\text{def}}{=} k^4 q^4 - \xi k^2 q^2 - 1 = (k^2 q^2 - \xi/2)^2 - (1 + \xi^2/4).$$

Equations (15) and (16) together constitute $F = (f_q, f_a)$.

4.2 The norm on the space of Fourier coefficients

Note that we diverge from [30] in the choice of our norm for the purpose of simplifying the exposition. The choice of norm is similar to [15], although we deviate from it slightly, again for the purposes of exposition.

Since the differential equation is analytic, the solution is going to be analytic as well and the coefficients will decay geometrically. This motivates us to work with the norm

$$\|a\|_{l^1_\nu} \stackrel{\text{def}}{=} \sum_{k=0}^{\infty} |a_k| \, \omega_k(\nu),$$

where the exponential weights are

$$\omega_k(\nu) = \omega_k \stackrel{\text{def}}{=} \begin{cases} 1 & k = 0 \\ 2\nu^k & k \geq 1, \end{cases}$$

for some $\nu > 1$ to be chosen when doing the final computer-assisted step of the proof (we suppress the dependence on ν in the notation for ω_k). We denote the corresponding Banach space by l^1_ν. In view of (13), this norm may also be written as

$$\|a\|_{l^1_\nu} = \sum_{k \in \mathbb{Z}} |a_{|k|}| \, \nu^{|k|}.$$

We endow the one-sided l^1_ν with the following extended discrete convolution product: given $a, b \in l^1_\nu$ the convolution product $a * b \in l^1_\nu$ has components

$$(a * b)_k \stackrel{\text{def}}{=} \sum_{k' \in \mathbb{Z}} a_{|k'|} b_{|k-k'|}.$$

This product satisfies the Banach algebra property

$$\|a * b\|_{l^1_\nu} \leq \|a\|_{l^1_\nu} \|b\|_{l^1_\nu}, \tag{17}$$

as can be checked directly (applying the triangle inequality):

$$\begin{aligned} \|a * b\|_{l^1_\nu} &= \sum_{k \in \mathbb{Z}} |(a*b)_{|k|}| \nu^{|k|} = \sum_{k,k' \in \mathbb{Z}} |a_{|k'|}| |b_{|k-k'|}| \nu^{|k|} \\ &\leq \sum_{k,k-k' \in \mathbb{Z}} |a_{|k'|}| \nu^{|k'|} |b_{|k-k'|}| \nu^{|k-k'|} = \|a\|_{l^1_\nu} \|b\|_{l^1_\nu}. \end{aligned}$$

In this notation the expression for $(f_a)_k$ in (16) reduces to

$$(f_a)_k = -\lambda_k(q) - (a * a * a)_k.$$

The dual of l^1_ν is $(l^1_\nu)^* \cong l^\infty_{\nu^{-1}} = \{(b_m)_{m=1}^\infty : \sup_{m\in\mathbb{N}} |b_m\omega_m^{-1}| < \infty\}$. Namely, for $b \in (l^1_\nu)^*$ we may use linearity to write

$$b(a) = \sum_{m\in\mathbb{N}} b(\delta^m)a_m,$$

where δ is the usual Knonecker delta:

$$\delta^m_k \stackrel{\text{def}}{=} \begin{cases} 1 & k = m \\ 0 & k \neq m. \end{cases}$$

Hence, writing $b_m \stackrel{\text{def}}{=} b(\delta^m)$ we obtain

$$|b(a)| = \left|\sum_{m=0}^\infty b_m a_m\right| = \left|\sum_{m=0}^\infty (b_m\omega_m^{-1})(a_m\omega_m)\right| \leq \sup_{m\in\mathbb{N}} |b_m\omega_m^{-1}| \sum_{m\in\mathbb{N}} |a_m|\omega_m.$$

We will identify $(l^1_\nu)^*$ with $l^\infty_{\nu^{-1}}$ and use

$$\|b\|_{(l^1_\nu)^*} \stackrel{\text{def}}{=} \sup_{m\in\mathbb{N}} |b(\delta^m)|\omega_m^{-1} = \sup_{m\in\mathbb{N}} |b_m|\omega_m^{-1}$$

Remark 7. *If $G \in B(l^1_\nu, l^1_\nu)$, then by linearity*

$$\begin{aligned}\|G(a)\|_{l^1_\nu} &= \sum_{k\in\mathbb{N}} |G(a)_k|\omega_k = \sum_{k,m\in\mathbb{N}} |G(\delta^m)_k a_m|\omega_k \\ &\leq \sum_{m\in\mathbb{N}} |a_m|\omega_m \sup_{m\in\mathbb{N}}\Big(\omega_m^{-1}\sum_{k\in\mathbb{N}} |G(\delta^m)_k|\omega_k\Big) = \|a\|_{l^1_\nu} \sup_{m\in\mathbb{N}} \omega_m^{-1}\|G(\delta^m)\|_{l^1_\nu}.\end{aligned}$$

Hence, writing $G_{km} \stackrel{\text{def}}{=} G(\delta^m)_k$, we obtain the explicit expression

$$\|G\|_{B(l^1_\nu,l^1_\nu)} = \sup_{m\in\mathbb{N}} \omega_m^{-1} \sum_{k\in\mathbb{N}} |G_{km}|\,\omega_k.$$

4.3 The product space

Since our unknowns are $x = (q, a)$, we use the product space $X = \mathbb{R} \times l^1_\nu$. We will use projections π_q and π_a onto $\mathbb{R}$ and l^1_ν, respectively. The trivial embedding of $\mathbb{R}$ and l^1_ν into X are both denoted by ι, since this will never cause confusion.

We fix a computational parameter $N \in \mathbb{N}$ (to be chosen when we do the final computer-assisted step of the proof, see §4.7). Given $x = (q, a) \in X$, we define the finite dimensional projection $\pi_N x = (q, a_0, \ldots, a_N) \in X_N \cong \mathbb{R} \times \mathbb{R}^{N+1} \cong \mathbb{R}^{N+2}$. We slightly abuse notation to write π_q and π_a for the projections from X_N onto $\mathbb{R}$ and $\mathbb{R}^{N+1}$, respectively: $\pi_q x_N = q$ and $\pi_a x_N = (a_k)_{k=0}^N$. The embedding of X_N into X by extending with zeros is again denoted by ι:

$$\pi_N \iota x_N = x_N \qquad \text{and} \qquad (\pi_a \iota x_N)_k = 0 \quad \text{for } k > N.$$

for all $x_N \in X_N$.

The truncated system, or Galerkin projection, is given by

$$F_N : X_N \to X_N, \qquad F_N(x_N) = \pi_N F(\iota x_N).$$

We solve $F_N = 0$ numerically (using a good initial guess and Newton's iteration method) to obtain an approximate zero $\overline{x}_N = (\overline{q}, \overline{a}_0, \ldots, \overline{a}_N)$ of F_N, and a corresponding approximate zero $\overline{x} = \iota\overline{x}_N$ of F. The Jacobian matrix

$$A^\dagger_N \stackrel{\text{def}}{=} DF_N(\overline{x}_N)$$

is inverted *numerically* to obtain

$$A_N \approx (A_N^\dagger)^{-1}.$$

Based on our expectation that the linear part in (16) will dominate for large k, the linear operators $A^\dagger$ and A are then built up as follows:

$$\pi_N(A^\dagger x) = A_N^\dagger \pi_N x \qquad \text{and} \qquad (\pi_a(A^\dagger x))_k = \lambda_k(\overline{q})(\pi_a x)_k \qquad \text{for } k > N \tag{18a}$$

$$\pi_N(Ax) = A_N \pi_N x \qquad \text{and} \qquad (\pi_a(Ax))_k = \lambda_k(\overline{q})^{-1}(\pi_a x)_k \qquad \text{for } k > N. \tag{18b}$$

We are now ready to define

$$T(x) \stackrel{\text{def}}{=} x - AF(x).$$

Remark 8. *Let Γ be a linear operator on X, then it can be decomposed into*

$$\Gamma = \begin{bmatrix} \Gamma_{qq} & \Gamma_{qa} \\ \Gamma_{aq} & \Gamma_{aa} \end{bmatrix}$$

with $\Gamma_{qq} \in \mathbb{R}$, $\Gamma_{qa} \in (l^1_\nu)^*$, $\Gamma_{aq} \in l^1_\nu$ and $\Gamma_{aa} \in B(l^1_\nu, l^1_\nu)$. Formally:

$$\pi_q \Gamma x = \Gamma_{qq}\pi_q x + \Gamma_{qa}\pi_a x$$
$$\pi_a \Gamma x = \Gamma_{aq}\pi_q x + \Gamma_{aa}\pi_a x.$$

We will use the same notation for bounded linear operators on X_N.

Remark 9. *Moreover, suppose $\Gamma \in L(X, X)$ is of the form*

$$\pi_N \Gamma x = \Gamma_N \pi_N x \qquad \text{and} \qquad (\pi_a \Gamma x)_k = \gamma_k x_k \quad \text{for } k > N.$$

with $\sup_{k>N} |\gamma_k| = \hat{\gamma} < \infty$ given. Then $(\Gamma_{qa})_k$ and $(\Gamma_{aq})_k$ vanish for $k > N$, hence their norms are computable, and

$$\|\Gamma_{aa}\|_{B(l^1_\nu, l^1_\nu)} = \max\left\{ \hat{\gamma}\,,\ \max_{0\le m\le N} \frac{1}{\omega_m} \sum_{k=0}^{N} |(\Gamma_{aa})_{km}|\omega_k \right\}$$

is also computable.

Remark 10. *We choose the truncation dimension $N \geq \widehat{N}(\overline{q}, \xi)$, where*

$$\widehat{N}(\overline{q}, \xi) \stackrel{\text{def}}{=} \frac{((1 + \xi^2/4)^{1/2} + \xi/2)^{1/2}}{\overline{q}},$$

so that

$$0 < \lambda_{N+1}(\overline{q}) \leq \lambda_k(\overline{q}) \quad \text{for all } k \geq N + 1. \tag{19}$$

This ensures both that the factor $\lambda_k(\overline{q})^{-1}$ in (18b) is well-defined for all $k > N$, and that A is of the form discussed in Remark 9 with $\hat{\gamma} = \lambda_{N+1}(\overline{q})^{-1}$.

4.4 The radii polynomials

Since we work on a product space, we are going to deviate somwehat from the setup in §2.3 and [30]. For $r = (r_1, r_2)$ with $r_1, r_2 > 0$ we define the *rectangle*

$$\mathcal{B}_r = \mathcal{B}_r(\overline{x}) = \{x \in X : |\pi_q(x - \overline{x})| \leq r_1, \|\pi_a(x - \overline{x})\|_{l^1_\nu} \leq r_2\}.$$

We will establish bounds (with D_q and D_a denoting partial derivatives)

$$|\pi_q T(\overline{x})| \leq Y_1 \tag{20a}$$

$$\|\pi_a T(\overline{x})\|_{l^1_\nu} \leq Y_2 \tag{20b}$$

$$\|D_q \pi_q T(x)\|_{B(\mathbb{R},\mathbb{R})} \leq Z_{11}(r) \qquad \text{for all } x \in \mathcal{B}_r, \tag{20c}$$

$$\|D_a \pi_q T(x)\|_{B(l^1_\nu,\mathbb{R})} \leq Z_{12}(r) \qquad \text{for all } x \in \mathcal{B}_r, \tag{20d}$$

$$\|D_q \pi_a T(x)\|_{B(\mathbb{R},l^1_\nu)} \leq Z_{21}(r) \qquad \text{for all } x \in \mathcal{B}_r, \tag{20e}$$

$$\|D_a \pi_a T(x)\|_{B(l^1_\nu,l^1_\nu)} \leq Z_{22}(r) \qquad \text{for all } x \in \mathcal{B}_r, \tag{20f}$$

for some $Y_1, Y_2 \in \mathbb{R}^+$ and $Z_{ij} : \mathbb{R}^+ \to \mathbb{R}^+$ for $i, j \in \{1, 2\}$. Clearly in (20c)-(20e) one should read $B(\mathbb{R}, \mathbb{R}) = \mathbb{R}$, $B(l^1_\nu, \mathbb{R}) = (l^1_\nu)^*$ and $B(\mathbb{R}, l^1_\nu) = l^1_\nu$. Then the *two radii polynomials* for our problem are

$$p_1(r_1, r_2) = Y_1 + r_1[Z_{11}(r_1, r_2) - 1] + r_2 Z_{12}(r_1, r_2) \tag{21a}$$
$$p_2(r_1, r_2) = Y_2 + r_1 Z_{21}(r_1, r_2) + r_2[Z_{22}(r_1, r_2) - 1]. \tag{21b}$$

We need to find an $\hat{r} = (\hat{r}_1, \hat{r}_2) > 0$ such that $p(\hat{r}) < 0$ component-wise, i.e.,

$$p_1(\hat{r}_1, \hat{r}_2) < 0 \qquad \text{and} \qquad p_2(\hat{r}_1, \hat{r}_2) < 0. \tag{22}$$

Theorem 11. *Assume that Y and Z satisfy the bounds* (20)*. Let p_1 and p_2 be the radii polynomials defined in* (21)*. If $\hat{r}_1, \hat{r}_2 > 0$ are such that the inequalities* (22) *are satisfied, then T has a unique fixed point in $\mathcal{B}_{\hat{r}}(\overline{x})$.*

Proof. To show that T maps $\mathcal{B}_{\hat{r}}(\overline{x})$ into itself, we use arguments similar to the ones in §2.5. Namely, let $x = (q, a) \in \mathcal{B}_{\hat{r}}(\overline{q}, \overline{a})$. To simplify notation, define the projected balls

$$B^q \overset{\text{def}}{=} \{q \in \mathbb{R} : |q - \overline{q}| \le \hat{r}_1\} \qquad \text{and} \qquad B^a \overset{\text{def}}{=} \{a \in l^1_\nu : \|a - \overline{a}\|_{l^1_\nu} \le \hat{r}_2\},$$

so that $\mathcal{B}_{\hat{r}}(\overline{x}) = B^q \times B^a$. Then, by applying the triangle inequality and the intermediate value theorem, we obtain

$$\begin{aligned}
\left|\pi_q T(q, a) - \overline{q}\right| &\le \left|\pi_q[T(q, a) - T(q, \overline{a})]\right| + \left|\pi_q[T(q, \overline{a}) - T(\overline{q}, \overline{a})]\right| + \left|\pi_q T(\overline{q}, \overline{a}) - \overline{q}\right| \\
&\le \sup_{a' \in B^a} \|D_a \pi_q T(q, a')\|_{(l^1_\nu)^*} \|a' - \overline{a}\|_{l^1_\nu} + \sup_{q' \in B^q} |D_q \pi_q T(q', \overline{a})| \, |q' - q| \; + \; Y_1 \\
&\le Z_{12}(\hat{r})\hat{r}_2 + Z_{11}(\hat{r})\hat{r}_1 + Y_1.
\end{aligned}$$

Since $p_1(\hat{r}) < 0$ by assumption, it follows that $|\pi_q T(q, a) - \overline{q}| < \hat{r}_1$. By an analogous argument, $\|\pi_a T(q, a) - \overline{a}\|_{l^1_\nu} < \hat{r}_2$. Hence T maps $\mathcal{B}_{\hat{r}}(\overline{x})$ into itself.

To show that T is a contraction mapping on $\mathcal{B}_{\hat{r}}(\overline{x})$ we need to choose a norm on the product space $X = \mathbb{R} \times l^1_\nu$. It turns out that T contracts with respect to the *weighted norm*

$$\|(q, a)\|_X \overset{\text{def}}{=} \max\{q/\hat{r}_1, \|a\|_{l^1_\nu}/\hat{r}_2\}. \tag{23}$$

Indeed, let $x_1, x_2 \in B_{\hat{r}}(\overline{x})$, then, by applying the mean value theorem and the triangle inequality,

$$\begin{aligned}
|\pi_q[T(x_1) - T(x_2)]| &\le \sup_{x' \in B_{\hat{r}}(\overline{x})} |D_q \pi_q T(x')| \, |\pi_q(x_1 - x_2)| \\
&\qquad + \sup_{x' \in B_{\hat{r}}(\overline{x})} \|D_a \pi_q T(x')\|_{(l^1_\nu)^*} \|\pi_a(x_1 - x_2)\|_{l^1_\nu} \\
&\le [Z_{11}(\hat{r})\hat{r}_1 + Z_{12}(\hat{r})\hat{r}_2] \, \|x_1 - x_2\|_X,
\end{aligned}$$

and analogously

$$\|\pi_a[T(x_1) - T(x_2)]\|_{l^1_\nu} \le [Z_{21}(\hat{r})\hat{r}_1 + Z_{22}(\hat{r})\hat{r}_2] \, \|x_1 - x_2\|_X.$$

From the above estimates we conclude that

$$\|T(x_1) - T(x_2)\|_X \le \max\big\{Z_{11}(\hat{r}) + Z_{12}(\hat{r})\hat{r}_2/\hat{r}_1, Z_{21}(\hat{r})\hat{r}_1/\hat{r}_2 + Z_{22}(\hat{r})\big\} \|x_1 - x_2\|_X. \tag{24}$$

It follows from the negativity of both radii polynomials (21) that the contraction rate

$$\max\big\{Z_{11}(\hat{r}) + Z_{12}(\hat{r})\hat{r}_2/\hat{r}_1, Z_{21}(\hat{r})\hat{r}_1/\hat{r}_2 + Z_{22}(\hat{r})\big\} \tag{25}$$

is less than unity. □

Theorem 12. *Suppose the assumptions of Theorem 11 are met. Then the unique fixed point $\hat{x} = (\hat{q}, \hat{a})$ obtained in Theorem 11 corresponds to a zero of F, hence $\hat{a}$ corresponds, via* (12)*, to a $2\pi/\hat{q}$-periodic solution of* (10) *with energy $E = 0$.*

Proof. The only thing left is to prove is injectivity of A, which is *automatic* from the negativity of the radii polynomials. Indeed, since $\lambda_k(\overline{q}) \neq 0$ for $k > N$ by (19), injectivity of A is equivalent to injectivity of A_N. The latter could be checked numerically, but that is not needed, since by the arguments in the proof of Theorem 11, negativity of the radii polynomials for $r = \hat{r}$ implies that $\|(I - ADF(\overline{x}))v\|_X < \|v\|_X$ for all $v \in X$, where the norm on X is given by (23). Namely, it follows from (24) that the operator norm $\|I - ADF(\overline{x})\|_{B(X,X)}$ is bounded by the expression (25), which is less than unity. Specializing to $v = \iota v_N$ one finds, for the induced finite dimensional norm $\|x_N\|_{X_N} = \|\iota x_N\|_X$, that $\|(I_N - A_N A_N^\dagger)v_N\|_{X_N} < \|v_N\|_{X_N}$ for all $v_N \in x_N$. This implies that A_N is invertible, hence A is injective. □

4.5 The estimates Y

Recalling (20a) and (20b), in this section establish the bounds

$$\begin{aligned} |\pi_q AF(\overline{x})| &\leq Y_1, \\ \|\pi_q AF(\overline{x})\|_{l^1_\nu} &\leq Y_2. \end{aligned}$$

We have

$$f_q(\overline{x}) = -2\overline{q}^2 \sum_{m=1}^{N} m^2 \overline{a}_m - \frac{1}{\sqrt{2}} \left[\overline{a}_0 + 2 \sum_{m=1}^{N} \overline{a}_m \right]^2 + \frac{1}{\sqrt{2}} = 0,$$

$$(f_a)_k(\overline{x}) = \begin{cases} -\lambda_k(\overline{q})\overline{a}_k - (\overline{a} * \overline{a} * \overline{a})_k & k = 0, \dots, N \\ -(\overline{a} * \overline{a} * \overline{a})_k & k = N+1, \dots, 3N \\ 0 & k > 3N. \end{cases}$$

There are thus only finitely many non-vanishing terms. Hence we set

$$\begin{aligned} Y_1 &= \left| \pi_q A_N \pi_N F(\overline{x}) \right|, \\ Y_2 &= \sum_{k=0}^{N} \left| (\pi_a A_N \pi_N F(\overline{x}))_k \right| \omega_k + \sum_{k=N+1}^{3N} \lambda_k(\overline{q})^{-1} |(\overline{a} * \overline{a} * \overline{a})_k| \omega_k, \end{aligned}$$

computed using interval arithmetic to obtain rigorous upper bounds.

4.6 The estimates Z

In this section we construct bounds, see (20),

$$|D_q \pi_q T(x)| \leq Z_{11}(r) \qquad \text{for all } x \in \mathcal{B}_r, \tag{26a}$$

$$\|D_a \pi_q T(x)\|_{(l^1_\nu)^*} \leq Z_{12}(r) \qquad \text{for all } x \in \mathcal{B}_r, \tag{26b}$$

$$\|D_q \pi_a T(x)\|_{l^1_\nu} \leq Z_{21}(r) \qquad \text{for all } x \in \mathcal{B}_r, \tag{26c}$$

$$\|D_a \pi_a T(x)\|_{B(l^1_\nu, l^1_\nu)} \leq Z_{22}(r) \qquad \text{for all } x \in \mathcal{B}_r. \tag{26d}$$

We will write

$$\mathcal{B}_1 \stackrel{\text{def}}{=} \mathcal{B}_{(1,1)} = \{(q, a) \in X : |q - \overline{q}| \leq 1, \|a - \overline{a}\|_{l^1_\nu} \leq 1\}.$$

As already mentioned in §2.4, for each of the four derivatives in (26), we split $DT(\overline{x} + w)v$, where $w = (w_q, w_a) \in \mathcal{B}_r$ and $v = (v_q, v_a) \in \mathcal{B}_1$ are arbitrary, into three pieces:

$$DT(\overline{x} + w)v = [I - AA^\dagger]v - A[DF(\overline{x}) - A^\dagger]v - A[DF(\overline{x} + rw) - DF(\overline{x})]v. \tag{27}$$

By bounding these three terms separately, we will find bounds $Z_{ij}(r) = Z^0_{ij} + Z^1_{ij} + Z^2_{ij}(r)$, $i, j \in \{1, 2\}$. We note that the first two terms are independent of w.

4.6.1 The bounds Z^0

We infer from the definitions of A and $A^\dagger$ in (18) that the first term in (27) reduces to a finite dimensional operator:

$$[I - AA^\dagger]v = \iota[I_N - A_N A_N^\dagger]\pi_N v.$$

Let us write $\Gamma = I - AA^\dagger$, which is of the form discussed in Remark 9 with $\hat{\gamma} = 0$. With the notation introduced in Remark 8 it follows from Remark 9 that the computable numbers

$$\begin{aligned} Z^0_{11} &= |\Gamma_{qq}| \\ Z^0_{12} &= \|\Gamma_{qa}\|_{(l^1_\nu)^*} \\ Z^0_{21} &= \|\Gamma_{aq}\|_{l^1_\nu} \\ Z^0_{22} &= \|\Gamma_{aa}\|_{B(l^1_\nu, l^1_\nu)}, \end{aligned}$$

bound the respective components of $I - AA^\dagger$.

4.6.2 The bounds Z^1

For the second term in (27) we first compute, recalling that $A_N^\dagger = DF_N(\pi_N \overline{x})$,

$$[Df_q(\overline{x}) - \pi_q A^\dagger]v = -2\overline{q}^2 \sum_{m=N+1}^{\infty} m^2 (v_a)_m - \sqrt{2}\left(\overline{a}_0 + 2\sum_{m=1}^{N} \overline{a}_m\right)\left(2\sum_{m=N+1}^{\infty} (v_a)_m\right) \tag{28a}$$

$$([Df_a(\overline{x}) - \pi_a A^\dagger]v)_k = \begin{cases} -3\,(\overline{a} * \overline{a} * v_a^0)_k & \text{for } 0 \le k \le N \\ -3\,(\overline{a} * \overline{a} * v_a)_k & \text{for } k > N, \end{cases} \tag{28b}$$

where

$$(v_a^0)_k \stackrel{\text{def}}{=} \begin{cases} 0 & 0 \le k \le N \\ (v_a)_k & k > N. \end{cases}$$

We note that both right-hand sides in (28) are independent of v_q, which implies that $D_q f(\overline{x})\pi_q - A^\dagger \iota \pi_q = 0$, hence

$$Z^1_{11} = 0 \qquad \text{and} \qquad Z^1_{21} = 0.$$

We then estimate for all $v \in \mathcal{B}_1$, using the characterization of $(l^1_\nu)^*$ in §4.2,

$$\begin{aligned} \left|\sum_{m=N+1}^{\infty} (v_a)_m\right| &\le \sup_{m>N} \omega_m^{-1} \le \omega_{N+1} \\ \left|\sum_{m=N+1}^{\infty} m^2 (v_a)_m\right| &\le \sup_{m>N} m^2 \omega_m^{-1} \le \tfrac{1}{2} Q(\nu, N), \end{aligned}$$

where

$$Q(\nu, N) \stackrel{\text{def}}{=} \begin{cases} \frac{4}{(e \ln \nu)^2} & N + 1 \le 2/\ln(\nu) \\ 2(N+1)^2 \omega_{N+1} & N + 1 > 2/\ln(\nu). \end{cases}$$

We immediately see that ν should not be chosen too close to 1 as this would lead to a very large value for Q. We define bounds $d_N = (d_q, d_{a0}, \ldots, d_{aN})$ as follows:

$$d_q \stackrel{\text{def}}{=} \overline{q}^2 Q(\nu, N) + \sqrt{2}\,\omega_{N+1}^{-1}\left|\overline{a}_0 + 2\sum_{m=1}^{N} \overline{a}_m\right| \ge |[Df_q(\overline{x}) - \pi_q A^\dagger]v| \quad \text{for all } v \in \mathcal{B}_1,$$

and for $k = 0, \ldots, N$

$$d_{ak} \stackrel{\text{def}}{=} 3(|\overline{a} * \overline{a}| * \chi)_k \ge |([Df_a(\overline{x}) - \pi_a A^\dagger]v)_k| \quad \text{for all } v \in \mathcal{B}_1,$$

c_q^{10}	$-4\widetilde{w}_q \sum_{m=1}^{N} m^2 \overline{a}_m$	$\widetilde{c}_q^{10}$	$-4\overline{q}\widetilde{w}_q \sum_{m=1}^{\infty} m^2 (v_a)_m$
c_q^{01}	$-4\overline{q} \sum_{m=1}^{\infty} m^2 (\widetilde{w}_a)_m$	$\widetilde{c}_q^{01}$	$-\sqrt{2}\left((\widetilde{w}_a)_0 + 2\sum_{m=1}^{\infty}(\widetilde{w}_a)_m\right)\left((v_a)_0 + 2\sum_{m=1}^{\infty}(v_a)_m\right)$
		$\widetilde{c}_q^{20}$	$-2\widetilde{w}_q^2 \sum_{m=1}^{\infty} m^2 (v_a)_m$
c_q^{11}	$-4\widetilde{w}_q \sum_{m=1}^{\infty} m^2 (\widetilde{w}_a)_m$		
c_{ak}^{10}	$-2k^2\widetilde{w}_q\big(6k^2\overline{q}^2 - \xi\big)\overline{a}_k$	$\widetilde{c}_{ak}^{10}$	$-2k^2\widetilde{w}_q\big(2k^2\overline{q}^3 - \xi\overline{q}\big)(v_a)_k$
c_{ak}^{01}	$-2k^2\big(2k^2\overline{q}^3 - \xi\overline{q}\big)(\widetilde{w}_a)_k$	$\widetilde{c}_{ak}^{01}$	$-6\,(\overline{a} * \widetilde{w}_a * v_a)_k$
c_{ak}^{20}	$-12k^4\widetilde{w}_q^2\overline{q}\overline{a}_k$	$\widetilde{c}_{ak}^{20}$	$-k^2\widetilde{w}_q^2\big(6k^2\overline{q}^2 - \xi\big)(v_a)_k$
c_{ak}^{11}	$-2k^2\widetilde{w}_q\big(6k^2\overline{q}^2 - \xi\big)(\widetilde{w}_a)_k$		
		$\widetilde{c}_{ak}^{02}$	$-3\,(\widetilde{w}_a * \widetilde{w}_a * v_a)_k$
c_{ak}^{30}	$-4k^4\widetilde{w}_q^3\overline{a}_k$	$\widetilde{c}_{ak}^{30}$	$-4k^4\widetilde{w}_q^3\overline{q}(v_a)_k$
c_{ak}^{21}	$-12k^4\widetilde{w}_q^2\overline{q}(\widetilde{w}_a)_k$		
		$\widetilde{c}_{ak}^{40}$	$-k^4\widetilde{w}_q^4(v_a)_k$
c_{ak}^{31}	$-4k^4\widetilde{w}_q^3(\widetilde{w}_a)_k$		

Table 1: The non-zero coefficients in the expansions (29).

where

$$\chi_k = \begin{cases} 0 & 0 \le k \le N \\ \omega_k^{-1} & N+1 \le k \le 3N \\ 0 & k > 3N, \end{cases}$$

and where absolute values in $|\overline{a} * \overline{a}|$ are taken component-wise. For $k > N$ we note that

$$|(\pi_a A[Df(\overline{x}) - A^\dagger]v)_k| \le \lambda_k(\overline{q})^{-1}|3(\overline{a} * \overline{a} * v_a)_k|$$

Hence we may estimate, by using (17) and (19),

$$\sum_{k=N+1}^{\infty} |(\pi_a A[Df(\overline{x}) - A^\dagger]v)_k|\omega_k \le 3\lambda_{N+1}(\overline{q})^{-1}\|\overline{a} * \overline{a}\|_{l^1_\nu} \qquad \text{for all } v \in \mathcal{B}_1,$$

provided $N \ge \widehat{N}(\overline{q}, \xi)$. We thus set

$$\begin{aligned} Z_{21}^1 &= \pi_q |A_N| d_N \\ Z_{22}^1 &= \|\pi_a |A_N| d_N\|_{l^1_\nu} + 3\lambda_{N+1}(\overline{q})^{-1}\|\overline{a} * \overline{a}\|_{l^1_\nu}, \end{aligned}$$

where absolute values in $|A_N|$ are taken component-wise.

4.6.3 The bounds Z^2

The final term in (27) is expanded in powers of r_1 and r_2 by writing $w = (r_1\widetilde{w}_q, r_2\widetilde{w}_a)$ with $\widetilde{w} \in \mathcal{B}_1$:

$$[Df_q(\overline{x} + w) - Df_q(\overline{x})]v = v_q \sum_{i,j} c_q^{ij}(\overline{x}, \widetilde{w}) r_1^i r_2^j + \sum_{i,j} \widetilde{c}_q^{ij}(\overline{x}, v_a, \widetilde{w}) r_1^i r_2^j, \tag{29a}$$

$$\big([Df_a(\overline{x} + w) - Df_a(\overline{x})]v\big)_k = v_q \sum_{i,j} c_{ak}^{ij}(\overline{x}, \widetilde{w}) r_1^i r_2^j + \sum_{i,j} \widetilde{c}_{ak}^{ij}(\overline{x}, v_a, \widetilde{w}) r_1^i r_2^j, \tag{29b}$$

where we write $(c_a^{ij})_k = c_{ak}^{ij}$ for convenience. All sums are finite sums; the non-vanishing coefficients c_q^{ij} and c_{ak}^{ij} are listed in Table 1.

We now compute uniform bounds

$$C_q^{ij}(\overline{x}) \ge |c_q^{ij}(\overline{x}, \widetilde{w})| \qquad \text{for all } \widetilde{w} \in \mathcal{B}_1, \tag{30a}$$

$$\widetilde{C}_q^{ij}(\overline{x}) \ge |\widetilde{c}_q^{ij}(\overline{x}, v_a, \widetilde{w})| \qquad \text{for all } \widetilde{w} \in \mathcal{B}_1, \|v_a\|_{l^1_\nu} \le 1, \tag{30b}$$

$$C_{ak}^{ij}(\overline{x}) \ge |c_{ak}^{ij}(\overline{x}, \widetilde{w})| \qquad \text{for all } \widetilde{w} \in \mathcal{B}_1, \qquad 0 \le k \le N, \tag{30c}$$

$$\widetilde{C}_{ak}^{ij}(\overline{x}) \ge |\widetilde{c}_{ak}^{ij}(\overline{x}, v_a, \widetilde{w})| \qquad \text{for all } \widetilde{w} \in \mathcal{B}_1, \|v_a\|_{l^1_\nu} \le 1, \quad 0 \le k \le N. \tag{30d}$$

C_q^{10}	$4\left\lvert\sum_{m=1}^N m^2\overline{a}_m\right\rvert$	$\widetilde{C}_q^{10}$	$2\overline{q}Q_\nu$
C_q^{01}	$2\overline{q}Q_\nu$	$\widetilde{C}_q^{01}$	$\sqrt{2}$
		$\widetilde{C}_q^{20}$	Q_ν
C_q^{11}	$2Q_\nu$		
C_{ak}^{10}	$2k^2\left\lvert 6k^2\overline{q}^2-\xi\right\rvert\lvert\overline{a}_k\rvert$	$\widetilde{C}_{ak}^{10}$	$2k^2\left\lvert 2k^2\overline{q}^3-\xi\overline{q}\right\rvert\omega_k^{-1}$
C_{ak}^{01}	$2k^2\left\lvert 2k^2\overline{q}^3-\xi\overline{q}\right\rvert\omega_k^{-1}$	$\widetilde{C}_{ak}^{01}$	$6\lVert\overline{a}\rVert_{l^1_\nu}\omega_k^{-1}$
C_{ak}^{20}	$12k^4\overline{q}\lvert\overline{a}_k\rvert$	$\widetilde{C}_{ak}^{20}$	$k^2\left\lvert 6k^2\overline{q}^2-\xi\right\rvert\omega_k^{-1}$
C_{ak}^{11}	$2k^2\left\lvert 6k^2\overline{q}^2-\xi\right\rvert\omega_k^{-1}$		
		$\widetilde{C}_{ak}^{02}$	$3\omega_k^{-1}$
C_{ak}^{30}	$4k^4\lvert\overline{a}_k\rvert$	$\widetilde{C}_{ak}^{30}$	$4k^4\overline{q}\omega_k^{-1}$
C_{ak}^{21}	$12k^4\overline{q}\omega_k^{-1}$		
		$\widetilde{C}_{ak}^{40}$	$k^4\omega_k^{-1}$
C_{ak}^{31}	$4k^4\omega_k^{-1}$		

Table 2: The uniform bounds $C(\overline{x})$ and $\widetilde{C}(\overline{x})$ on the coefficients $c(\overline{x},\widetilde{w})$ and $\widetilde{c}(\overline{x},v_a,\widetilde{w})$, see (30).

These are summarized in Table 2, using the notation

$$Q_\nu \stackrel{\text{def}}{=} \frac{4}{(e\ln\nu)^2} \geq 2\sum_{m\in\mathbb{N}} m^2|(v_a)_m| \qquad \text{for all } \|v_a\|_{l^1_\nu}\leq 1.$$

For $k > N$ we use that $N \geq \widehat{N}(\overline{q},\xi)$, see Remark 10, hence we obtain the bound

$$\mu_{N+1} \stackrel{\text{def}}{=} \frac{(N+1)^4}{\lambda_{N+1}(\overline{q})} \geq \frac{k^4}{\lambda_k(\overline{q})} \qquad \text{for all } k \geq N+1.$$

This allows the uniform "tail" estimates

$$C^{ij}_{\text{tail}}(\overline{x}) \geq \sum_{k>N}\left|\lambda_k(\overline{q})^{-1}c^{ij}_{ak}(\overline{x},\widetilde{w})\right|\omega_k \qquad \text{for all } \widetilde{w}\in\mathcal{B}_1, \tag{31a}$$

$$\widetilde{C}^{ij}_{\text{tail}}(\overline{x}) \geq \sum_{k>N}\left|\lambda_k(\overline{q})^{-1}\widetilde{c}^{ij}_{ak}(\overline{x},v_a,\widetilde{w})\right|\omega_k \qquad \text{for all } \widetilde{w}\in\mathcal{B}_1 \text{ and } \|v_a\|_{l^1_\nu}\leq 1, \tag{31b}$$

where the non-zero C^{ij}_{tail} and $\widetilde{C}^{ij}_{\text{tail}}$ are listed in Table 3.

Finally, with the notation $C^{ij}_N = (C^{ij}_q, C^{ij}_{a0},\ldots,C^{ij}_{aN})$ and $\widetilde{C}^{ij}_N = (\widetilde{C}^{ij}_q, \widetilde{C}^{ij}_{a0},\ldots,\widetilde{C}^{ij}_{aN})$, we set

$$\begin{aligned}
Z^2_{11}(r_1,r_2) &= \sum_{i,j}\pi_q|A_N|C^{ij}_N\, r_1^i r_2^j\\
Z^2_{12}(r_1,r_2) &= \sum_{i,j}\pi_q|A_N|\widetilde{C}^{ij}_N\, r_1^i r_2^j\\
Z^2_{21}(r_1,r_2) &= \sum_{i,j}\left\|\pi_a|A_N|C^{ij}_N\right\|_{l^1_\nu} r_1^i r_2^j + \sum_{i,j} C^{ij}_{\text{tail}}\, r_1^i r_2^j\\
Z^2_{22}(r_1,r_2) &= \sum_{i,j}\left\|\pi_a|A_N|\widetilde{C}^{ij}_N\right\|_{l^1_\nu} r_1^i r_2^j + \sum_{i,j} \widetilde{C}^{ij}_{\text{tail}}\, r_1^i r_2^j.
\end{aligned}$$

All sums are over (a subset of) $0\leq i\leq 4$, $0\leq j\leq 2$.

4.7 Success

The estimates from §4.5 and §4.6, as well as the radii polynomials (22) have been implemented in the Matlab code `SHproof.m`, which uses the interval arithmetic package Intlab [23]. Based on Theorems 11 and 12 the script `runproof.m` successfully proves the existence aspect (as discussed at the end of §3) of Theorem 6 for $\xi = 0.01j$ for $j = 0,1,\ldots,203$. We use $N = 20$ and $\nu = 1.5$. These choices were made after some experimentation with the code. The code can be found at `http://www.few.vu.nl/~janbouwe/code/AMSnotes/`

		$\widetilde{C}^{10}_{\text{tail}}$	$4\overline{q}^3\mu_{N+1}$
C^{01}_{tail}	$4\overline{q}^3\mu_{N+1}$	$\widetilde{C}^{01}_{\text{tail}}$	$6\lambda_{N+1}(\overline{q})^{-1}\|\overline{a}\|_{l^1_\nu}$
		$\widetilde{C}^{20}_{\text{tail}}$	$6\overline{q}^2\mu_{N+1}$
C^{11}_{tail}	$12\overline{q}^2\mu_{N+1}$		
		$\widetilde{C}^{02}_{\text{tail}}$	$3\lambda_{N+1}(\overline{q})^{-1}$
		$\widetilde{C}^{30}_{\text{tail}}$	$4\overline{q}\mu_{N+1}$
C^{21}_{tail}	$12\overline{q}\mu_{N+1}$		
		$\widetilde{C}^{40}_{\text{tail}}$	μ_{N+1}
C^{31}_{tail}	$4\mu_{N+1}$		

Table 3: The uniform norm bounds $C^{ij}_{\text{tail}}(\overline{x})$ and $\widetilde{C}^{ij}_{\text{tail}}(\overline{x})$ on the non-vanishing tail terms c^{ij}_{ak} and $\widetilde{c}^{ij}_{ak}$ for $k > N$, incorporating the left-multiplication by the diagonal part of A, see (31).

References

[1] Zin Arai, William Kalies, Hiroshi Kokubu, Konstantin Mischaikow, Hiroe Oka, and Paweł Pilarczyk. A database schema for the analysis of global dynamics of multiparameter systems. *SIAM J. Appl. Dyn. Syst.*, 8(3):757–789, 2009.

[2] Gianni Arioli and Hans Koch. Integration of dissipative partial differential equations: a case study. *SIAM J. Appl. Dyn. Syst.*, 9(3):1119–1133, 2010.

[3] Gianni Arioli and Hans Koch. Integration of dissipative partial differential equations: a case study. *SIAM J. Appl. Dyn. Syst.*, 9(3):1119–1133, 2010.

[4] B. Breuer, J. Horák, P. J. McKenna, and M. Plum. A computer-assisted existence and multiplicity proof for travelling waves in a nonlinearly supported beam. *J. Differential Equations*, 224(1):60–97, 2006.

[5] CAPD: Computer assisted proofs in dynamics, a package for rigorous numerics. `http://capd.ii.uj.edu.pl/`.

[6] R. Castelli and J.-P. Lessard. Rigorous numerics in Floquet theory: computing stable and unstable bundles of periodic orbits. *SIAM Journal on Applied Dynamical Systems*, 12:204–245, 2013.

[7] Charles Conley. *Isolated invariant sets and the Morse index*, volume 38 of *CBMS Regional Conference Series in Mathematics*. American Mathematical Society, Providence, R.I., 1978.

[8] M. C. Cross and P. C. Hohenberg. Pattern formation outside of equilibrium. *Rev. Mod. Phys.*, 65(3):851–1112, Jul 1993.

[9] S. Day and W.D. Kalies. Rigorous computation of the global dynamics of integrodifference equations with smooth nonlinearities. *SIAM Journal on Numerical Analysis*, 51:2957–2983, 2013.

[10] S. Day, J.P. Lessard, and K. Mischaikow. Validated continuation for equilibria of PDEs. *SIAM J. Numer. Anal*, 45(4):13981424, 2007.

[11] R. L. Devaney. Homoclinic orbits in Hamiltonian systems. *J. Differential Equations*, 21(2):431–438, 1976.

[12] M. Gameiro and J.-P. Lessard. Efficient rigorous numerics for higher-dimensional PDEs via one-dimensional estimates. *SIAM Journal on Numerical Analysis*, 51:2063–2087, 2013.

[13] R. W. Ghrist, J. B. van den Berg, and R. C. Vandervorst. Morse theory on spaces of braids and Lagrangian dynamics. *Invent. Math.*, 152(2):369–432, 2003.

[14] Thomas C. Hales. A proof of the Kepler conjecture. *Ann. of Math. (2)*, 162(3):1065–1185, 2005.

[15] A. Hungria, J.P. Lessard, and J.D. Mireles-James. Rigorous numerics for analytic solutions of differential equations: the radii polynomial approach, 2014. Preprint.

[16] W. D. Kalies, J. Kwapisz, and R. C. A. M. VanderVorst. Homotopy classes for stable connections between Hamiltonian saddle-focus equilibria. *Comm. Math. Phys.*, 193(2):337–371, 1998.

[17] W.D. Kalies, K. Mischaikow, and R.C.A.M. van der Vorst. Lattice structures for attractors I. *Journal of Computational Dynamics*, 1:307–338, 2014.

[18] Oscar E. Lanford, III. A computer-assisted proof of the Feigenbaum conjectures. *Bull. Amer. Math. Soc. (N.S.)*, 6(3):427–434, 1982.

[19] Jean-Philippe Lessard and Christian Reinhardt. Rigorous numerics for nonlinear differential equations using chebyshev series. *SIAM J. Numer. Anal.*, 52(1):1–22, 2014.

[20] Tien Yien Li and James A. Yorke. Period three implies chaos. *Amer. Math. Monthly*, 82(10):985–992, 1975.

[21] M. T. Nakao. Numerical verification methods for solutions of ordinary and partial differential equations. *Numer. Funct. Anal. Optim.*, 22(3-4):321–356, 2001.

[22] Neil Robertson, Daniel Sanders, Paul Seymour, and Robin Thomas. The four-colour theorem. *J. Combin. Theory Ser. B*, 70(1):2–44, 1997.

[23] L.N. Rump. INTLAB - INTerval LABoratory. In Tibor Csendes, editor, *Developments in Reliable Computing*, pages 77–104. Kluwer Academic Publishers, Dordrecht, 1999. `http://www.ti3.tuhh.de/rump/`.

[24] Dietmar Salamon. Morse theory, the Conley index and Floer homology. *Bull. London Math. Soc.*, 22(2):113–140, 1990.

[25] A.N. Sharkovskii. Co-existence of cycles of a continuous mapping of the line into itself. *Ukrainian Math. J.*, 16:61–71, 1964.

[26] L. P. Shil'nikov. A case of the existence of a denumerable set of periodic motions. *Dokl. Akad. Nauk SSSR*, 160:558–561, 1965.

[27] J. Swift and P. C. Hohenberg. Hydrodynamic fluctuations at the convective instability. *Phys. Rev. A*, 15(1):319–328, Jan 1977.

[28] W. P. Thurston. On the geometry and dynamics of diffeomorphisms of surfaces. *Bull. Amer. Math. Soc. (N.S.)*, 19(2):417–431, 1988.

[29] Warwick Tucker. A rigorous ODE Solver and Smale's 14th Problem. *Foundations of Computational Mathematics*, 2(1):53–117–117, 2002-12-21.

[30] Jan Bouwe van den Berg and Jean-Philippe Lessard. Chaotic braided solutions via rigorous numerics: chaos in the Swift-Hohenberg equation. *SIAM J. Appl. Dyn. Syst.*, 7(3):988–1031, 2008.

[31] Jan Bouwe van den Berg, Jean-Philippe Lessard, and Konstantin Mischaikow. Global smooth solution curves using rigorous branch following. *Math. Comp.*, 79(271):1565–1584, 2010.

[32] J.B. van den Berg, A. Deschnes, J.-P. Lessard, and J.D. Mireles James. Stationary coexistence of hexagons and rolls via rigorous computations. *SIAM Journal on Applied Dynamical Systems*, 14:942–979, 2015.

[33] J.B. van den Berg, C. M. Groothedde, and J. F. Williams. Rigorous computation of a radially symmetric localized solution in a ginzburg–landau problem. *SIAM J. Appl. Dyn. Syst.*, 14(1):423–447, 2015.

[34] Piotr Zgliczyński. Rigorous numerics for dissipative partial differential equations. II. Periodic orbit for the Kuramoto-Sivashinsky PDE—a computer-assisted proof. *Found. Comput. Math.*, 4(2):157–185, 2004.

[35] Piotr Zgliczyński. Covering relations, cone conditions and the stable manifold theorem. *Journal of Differential Equations*, 246(5):1774 – 1819, 2009.